Influence of Hall effect and toroidal flow on the plasmoid formation and incomplete reconnection in the low resistivity plasma in Tokamak

W. Zhang[1], Z. W. Ma[1,*], and H. W. Zhang[1]

[1]Institute for Fusion Theory and Simulation, Department of Physics, Zhejiang University, Hangzhou 310027, China

Abstract: The nonlinear resistive-kink mode in the low resistivity plasma in Tokamak is investigated through the three-dimensional, toroidal, and nonlinear Hall-MHD code CLT. It is found that, without the two-fluid effect and the toroidal flow, the system can evolve into a steady-state with the saturated main m/n=1/1 magnetic island and the co-existing large secondary island. The main m/n=1/1 magnetic island cannot push the hot core plasma out of the q=1 surface as it does in Kadomstev's model, and the reconnection is incomplete. However, with the two-fluid effect or the toroidal flow, the nonlinear behaviors of the resistive-kink mode could be essentially different. The two-fluid effect and the toroidal flow can break the symmetry during the plasmoid formation, which destroys the balance between the main m/n=1/1 magnetic island and the large secondary island. The large secondary island is then merged into the main m/n=1/1 island. After that, the main m/n=1/1 island finally occupies the whole mix region, and all magnetic flux in the mix region is reconnected.

[a)] Corresponding Author: zwma@zju.edu.cn

I. Introduction

Sawteeth are often observed in Tokamaks when the central safety factor, q, approaches or falls below unity in the plasma core [1-6]. A sawtooth cycle consists of a slow ramp, during which the plasma temperature profile peaks in the core region, and a rapid relaxation, also called the sawtooth crash, during which the temperature profile is rapidly flattened. Sawteeth are dangerous for Tokamak operations since they can flatten the plasma temperature and trigger neo-classical tearing modes in nearby resonant surfaces [7, 8], which leads to significant degradation of energy confinement. However, the mechanism for sawteeth is not well understood, and it is still a hot issue up to now. [9-31]

It is widely believed that sawtooth oscillations are triggered by the resistive kink mode with m/n=1/1, where m and n are the poloidal and toroidal mode numbers. Kadomtsev proposed a "complete reconnection model" in 1975: an m/n=1/1 magnetic island begins to grow at the top of the sawtooth ramp and rapidly fills the entire core region. Consequently, the safety factor becomes larger than unity in the plasma core.[32] While experimental observations from small and low plasma temperature Tokamaks corroborate Kadomstev's theory [1], the crash time in large and hot Tokamaks [4, 5] is much shorter than Kadomstev's prediction. By including the two-fluid effect[33-37], the electron inertia effect[38], and the stochasticity of the magnetic field[39], and considering the ideal MHD instabilities[40-42], the crash time can be much shorter than Kadomstev's prediction and agrees well with experimental observations.

It should be noted that the plasma is sometimes observed to behave differently from the "complete reconnection model", for example, in the experimental observations presented in Refs. [5, 43, 44], the m/n=1/1 island persists for long periods during sawtooth ramps, and the central safety factor stays below unity after the sawtooth crash. This situation has prompted the formulation of a semi-heuristic "incomplete reconnection model", a discussion of which can be found in Ref. [45]. Another incomplete reconnection model was proposed by Beidler et al. [46], who suggested that

the incomplete reconnection is due to the increase of the electron diamagnetic frequency at the X-point of the *m/n*=1 magnetic island. However, neither of the two incomplete reconnection models has been self-consistently corroborated by numerical simulations.

Another incomplete reconnection model proposed by Yu et al. [47] is corroborated through the reduced-MHD model in the simple cylindrical geometry. They found that when the Lundquist number S is sufficiently large, plasmoids form during the nonlinear evolution of the *m/n*=1/1 resistive-kink mode and merge into a large secondary island, which can stop the reconnection process and lead to the incomplete reconnection. While Yu's model is promising to reveal the incomplete reconnection sawteeth, further efforts are necessary to explore the validation of the model in a more realistic tokamak configuration, using the full-MHD equations and including two-fluid effect and plasma rotations. In the present paper, we perform the simulation studies to investigate the dynamics of plasmoids during a sawtooth oscillation in the tokamak geometry using the 3D toroidal nonlinear Hall-MHD code CLT.[48]

The remainder of the paper is organized as follows: the numerical model is given in Section. II. In Section III. A, we numerically investigate the nonlinear evolution of the resistive-kink mode in Tokamak through resistive-MHD simulation. In Section III. B and C, the influence of the Hall effect and the toroidal flow are studied. A discussion has given in Section IV.

II. Numerical model

In dimensionless units, the 3D toroidal Hall-MHD equations used in CLT are given as follows:

$$\frac{\partial \rho}{\partial t} = -\nabla \cdot (\rho \mathbf{v}) + \nabla \cdot [D \nabla (\rho)], \tag{1}$$

$$\frac{\partial p}{\partial t} = -\mathbf{v} \cdot \nabla p - \Gamma p \nabla \cdot \mathbf{v} + \nabla \cdot [\kappa_{\perp} \nabla (p - p_0)] + \nabla \cdot [\kappa_{\parallel} \nabla_{\parallel} p], \tag{2}$$

$$\frac{\partial \mathbf{v}}{\partial t} = -\mathbf{v} \cdot \nabla \mathbf{v} + (\mathbf{J} \times \mathbf{B} - \nabla p) / \rho + \nabla \cdot [\nu \nabla (\mathbf{v})], \tag{3}$$

$$\frac{\partial \mathbf{B}}{\partial t} = -\nabla \times \mathbf{E}, \tag{4}$$

$$\mathbf{E} = -\mathbf{v}\times\mathbf{B} + \eta(\mathbf{J}-\mathbf{J}_0) + \frac{d_i}{\rho}(\mathbf{J}\times\mathbf{B} - \nabla p_e), \tag{5}$$

$$\mathbf{J} = \nabla\times\mathbf{B}, \tag{6}$$

where ρ, p, p_e, $\mathbf{v}$, $\mathbf{J}$, $\mathbf{B}$, and $\mathbf{E}$ are the plasma density, the plasma pressure, the electron pressure, the fluid velocity, the current density, the magnetic field, and the electric field, respectively. The subscript "0" denotes the initial quantities. $\Gamma(=5/3)$ is the ratio of specific heat of the plasma. η, D, $\kappa_\perp$, $\kappa_\parallel$, and υ are the resistivity, the diffusion coefficient, the perpendicular and parallel thermal conductivity, and the viscosity, respectively. $d_i = c/\omega_{pi}$ is the ion inertial length, where ω_{pi} is the ion plasma frequency, and c is the speed of light. In the present paper, the ion temperature is assumed to be zero, i.e., $p = p_e$. As shown in our previous studies,[37, 49] the two-fluid effect is self-consistently included in the Hall-MHD equations, i.e. the electron diamagnetic frequency $\omega_{*e} = -\frac{d_i m}{\rho r B}\frac{dp_e}{dr}$ and the ion-sound Larmor radius $\rho_s = d_i\sqrt{\mu_0 p / B_0^2}$.

All the variables are normalized as follows: $\mathbf{x}/a \to \mathbf{x}$, $t/t_A \to t$, $\rho/\rho_{00} \to \rho$, $p/(B_{00}^2/\mu_0) \to p$, $p_e/(B_{00}^2/\mu_0) \to p_e$, $\mathbf{v}/v_A \to \mathbf{v}$, $\mathbf{J}/(B_{00}/\mu_0 a) \to \mathbf{J}$, $\mathbf{B}/B_{00} \to \mathbf{B}$, $\mathbf{E}/(v_A B_{00}) \to \mathbf{E}$, $\eta/(\mu_0 a^2/t_A) \to \eta$, $D/(a^2/t_A) \to D$, $\kappa_\perp/(a^2/t_A) \to \kappa_\perp$, $\kappa_\parallel/(a^2/t_A) \to \kappa_\parallel$, $\nu/(a^2/t_A) \to \nu$, and $d_i/a \to d_i$, respectively. B_{00} and ρ_{00} are the initial magnetic field and the plasma density at the magnetic axis, respectively. a is the minor radius, $v_A = B_{00}/\sqrt{\mu_0\rho_{00}}$ is the Alfvén speed, and $t_A = a/v_A$ is the Alfvén time.

In CLT, the electric field is chosen to be an intermediate variable for the sake of keeping $\nabla\cdot\mathbf{B} = 0$. CLT's numerical scheme is the 4th order finite difference method for the spatial derivatives and the 4th order Runge–Kutta scheme for the time

integration. We choose the cut-cell method to handle the boundary problems since the physical boundary is not located at the grids [50]. In the present paper, the fixed boundary condition is used for all the variables.

III. Simulation results

A. Plasmoid formation and incomplete reconnection

Firstly, we follow the simulation studies by Yu et al. [47] in this subsection. We choose a similar initial equilibrium in our simulations. The function of the initial safety factor (q) profile is given as follows:

$$q = q_0 \times (1 + (\psi / q_1)^{q_2})^{\frac{1}{q_2}} \tag{7}$$

where $q_0 = 0.9$, $q_1 = 1.0$, and $q_2 = 1.0$. The q profile is shown in Figure 1, and the plasma beta is assumed to be $\beta \sim 0$. The radial position of the q=1 resonant surface is $r_1 = 0.34$, and the local magnetic shear is $s_1 = 0.2$.

The initial equilibrium is obtained from the NOVA code [51]. Mimicking a toroidal Tokamak configuration, the aspect ratio is chosen to be $R_0 / a = 3/1$. With $q_0 = 0.9$ (where q_0 is the safety factor at the magnetic axis), the most unstable mode is the m/n=1/1 resistive kink mode in the system. In order to investigate the secondary tearing instability, we choose a relatively low resistivity $\eta = 1.0 \times 10^{-7}$ in this subsection. Other parameters are chosen to be $D = 1.0 \times 10^{-4}$, $\kappa_\perp = 3.0 \times 10^{-6}$, $\kappa_\parallel = 5.0 \times 10^{-2}$, and $\nu = 1.0 \times 10^{-8}$. We switch off Hall/diamagnetic effects by choosing $d_i = 0$.

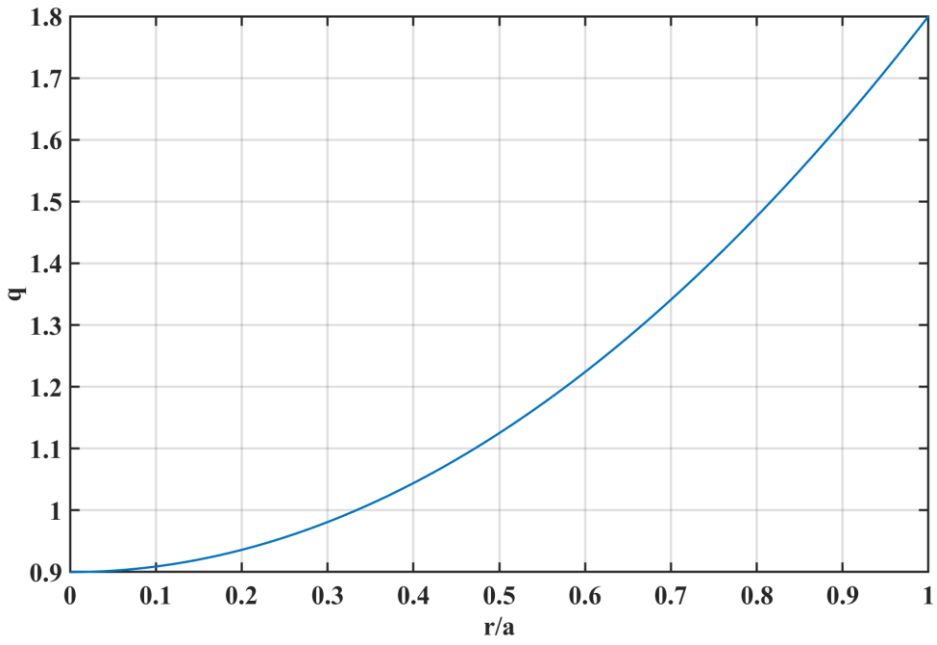

Figure 1 Initial q profile.

The evolutions of the kinetic energy and the growth rate of the resistive-kink mode are shown in Figure 2. The growth rate of the resistive-kink mode keeps unchanged during its linear growth and slowly reduces at the nonlinear stage, which is similar to the previous simulation studies of the complete reconnection sawtooth.[52] However, after $t > 4200t_A$, the dynamics are found to be qualitatively different from the well-known Kadomtsev's model[32], i.e., the growth rate of the resistive-kink mode increases evidently. This is because the secondary tearing instabilities occur when the current sheet is thinner than a critical value, which leads to the magnetic reconnection acceleration [47, 53].

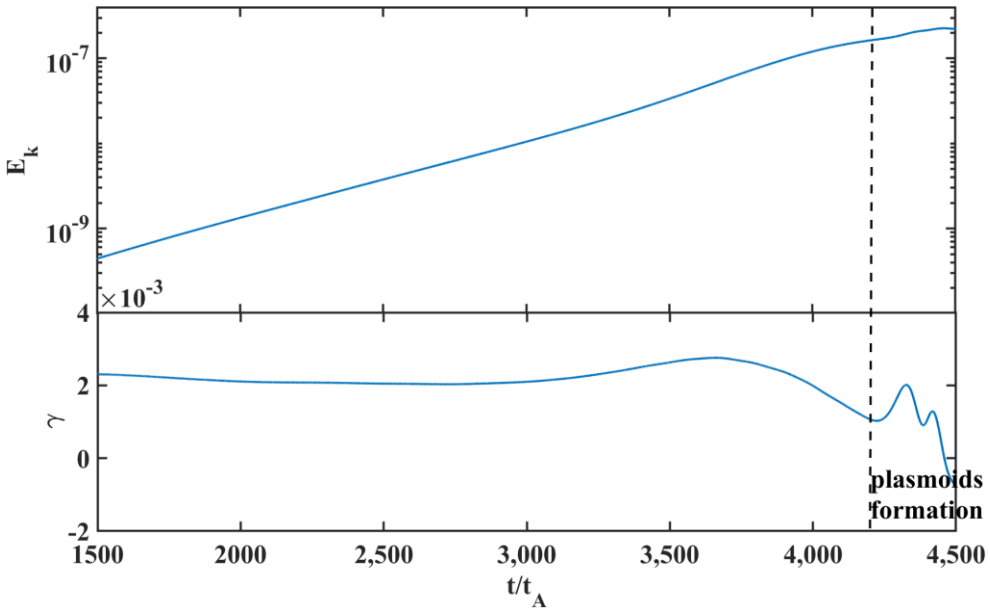

Figure 2 The evolutions of the kinetic energy and the growth rate of the resistive-kink mode.

The contour plots of the toroidal current density at the four typical moments ((a) $t = 3042t_A$ at the linear stage, (b) $t = 4069t_A$ at the early nonlinear stage, (c) $t = 4335t_A$ when the secondary tearing instability occurs, and (d) $t = 4487t_A$ when a large secondary island forms.) are shown in Figure 3. As we know, the nonlinear evolution of the resistive-kink mode can lead to a thin current sheet (e.g., Figure 3b). If the ratio of the current sheet's length to its thickness reaches a critical value, the current sheet becomes unstable to the secondary tearing instability.[54] The thin current sheet is then broken up (e.g., Figure 3c and d) with the development of the secondary tearing instability.

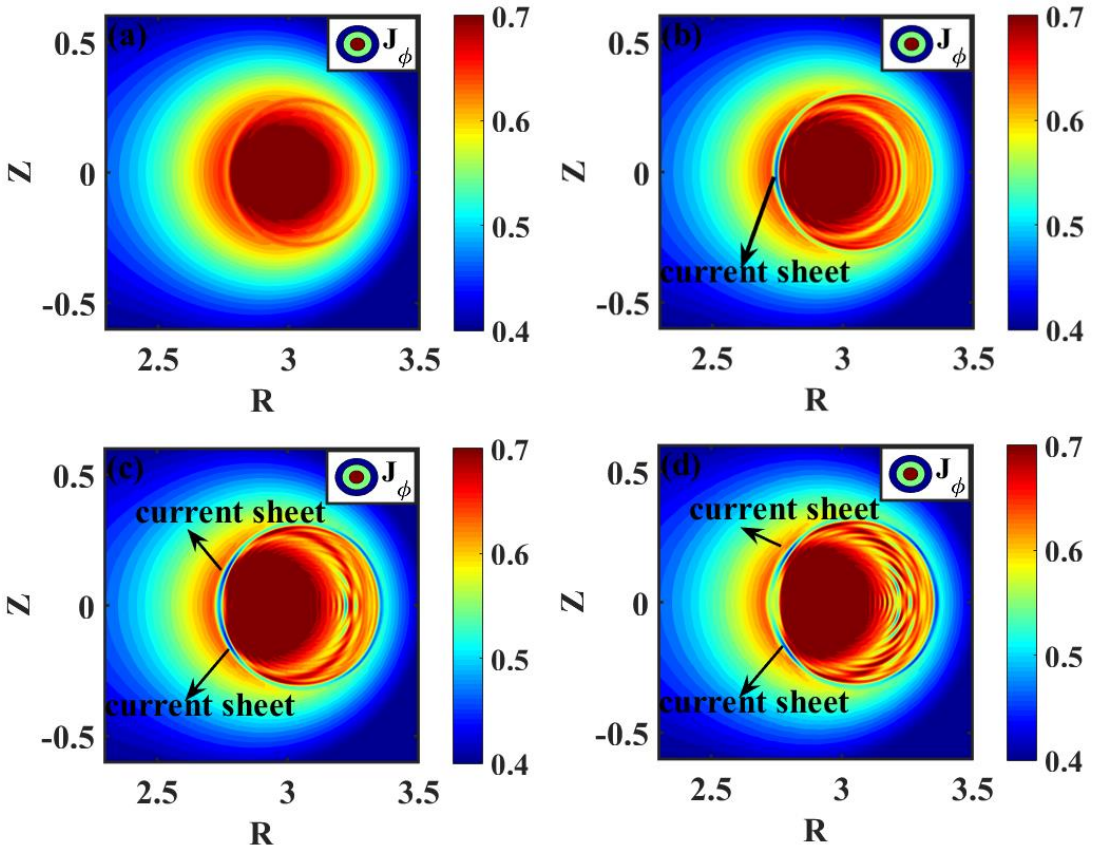

Figure 3 The contour plots of the toroidal current density at the four typical moments ((a) $t = 3042t_A$ at the linear stage, (b) $t = 4069t_A$ at the early nonlinear stage, (c) $t = 4335t_A$ when the secondary tearing instability occurs, and (d) $t = 4487t_A$ when a large secondary island forms).

The Poincare plots of the magnetic field simultaneously as Figure 3 are shown in Figure 4. With the development of the resistive-kink mode, a large m/n=1/1 magnetic island forms (Figure 4a and b). After the current sheet becomes unstable to the secondary tearing instability, the current sheet is broken up and the multiple X-points reconnection occurs (Figure 4c). Several secondary islands form in this process. These secondary islands merge into a large secondary island (Figure 4d). The large secondary island gradually prevents the hot core from shifting away from the central region, and the system then enters into a saturated state. The main *m/n*=1/1 magnetic island cannot fully occupy the whole mix region as it does in Kadomtsev's model, i.e., the reconnection process is "incomplete". It should be noted that the helicities of the

magnetic field lines will not change since the magnetic flux surfaces around the axis have not been destroyed. As a result, the safety factor at the magnetic axis will remain unchanged, i.e., $q_0 = 0.9$, throughout the simulation, which could be seen from the safety factor profiles in Figure 5.

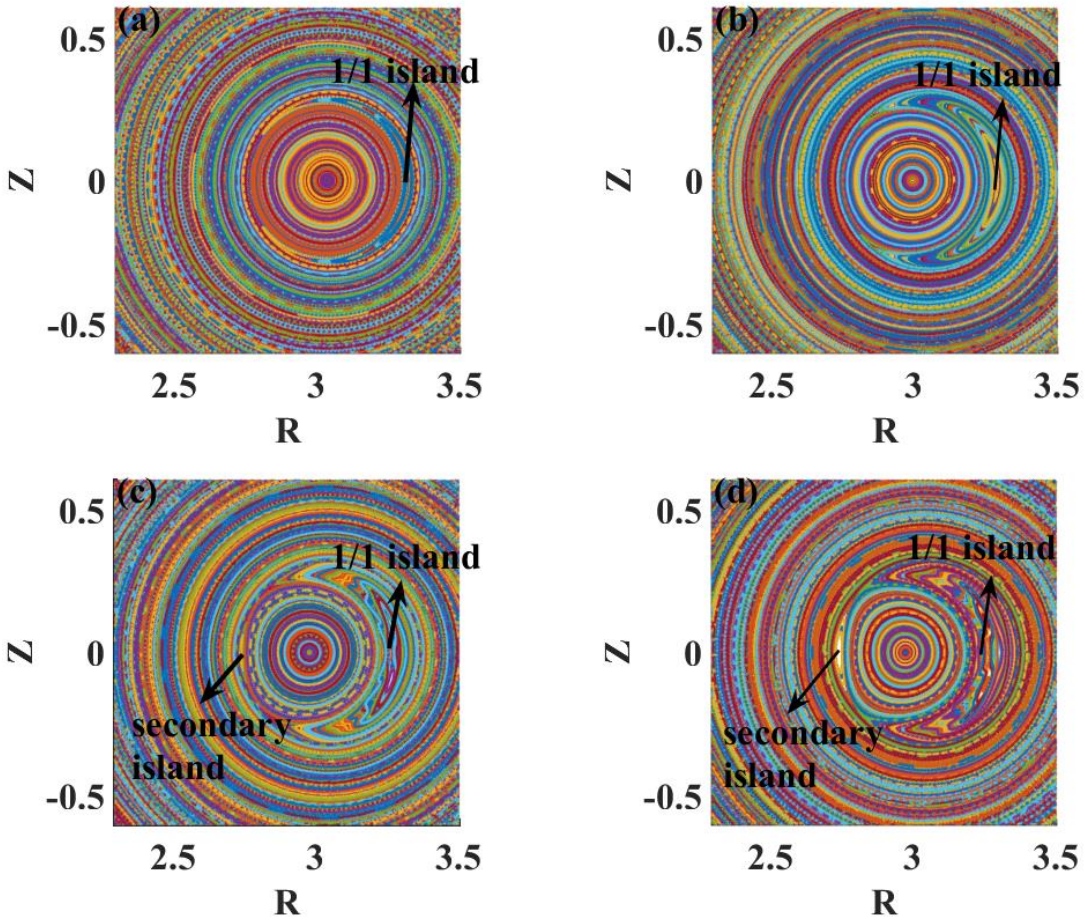

Figure 4 The Poincare plots of the magnetic field at the four typical moments ((a) $t = 3042t_A$ at the linear stage, (b) $t = 4069t_A$ at the early nonlinear stage, (c) $t = 4335t_A$ when the secondary tearing instability occurs, and (d) $t = 4487t_A$ when a large secondary island forms).

The safety factor profiles along the Z=0 plane at different times are shown in Figure 5. The system is unstable for the *m/n*=1/1 resistive-kink mode, an *m/n*=1/1 magnetic island forms at the linear stage ($t = 3042t_A$). During the early nonlinear evolution of the

resistive-kink mode, the *m/n*=1/1 island continues to grow up, and the magnetic shear at the X-point becomes larger and larger. A very thin current sheet forms at the X-point, which could also be seen in Figure 3. However, when the ratio of the current sheet's length to its thickness reaches a critical value, plasmoids form in this thin current sheet and then merge into a large secondary island. As a result, the safety factor profile becomes flattened at the previous X-point. In this region, q is equal to 1.0, which indicates that the large secondary island's helicity is *m/n*=1/1. It should also be noted that the safety factor at the magnetic axis stay $q_0 = 0.9$ throughout the simulation but the magnetic axis is shifted by the kink instability. The contour plot of the safety factor at the saturated stage is shown in Figure 6. As we can see, the 2D contour plot of q agrees well with the Poincare plots of the magnetic field lines (Figure 4), i.e., $q = 1.0$ inside the main *m/n*=1/1 island and the large secondary island, and $q < 1.0$ around the magnetic axis. The evolution of the safety factor profile also indicates that the reconnection is incomplete.

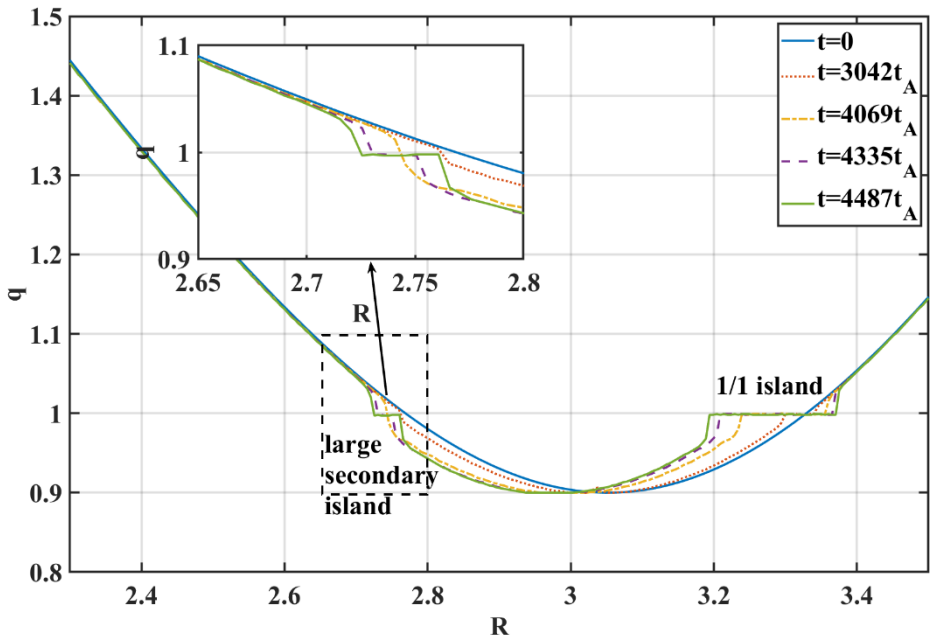

Figure 5 The safety factor profiles along the Z=0 plane at different times.

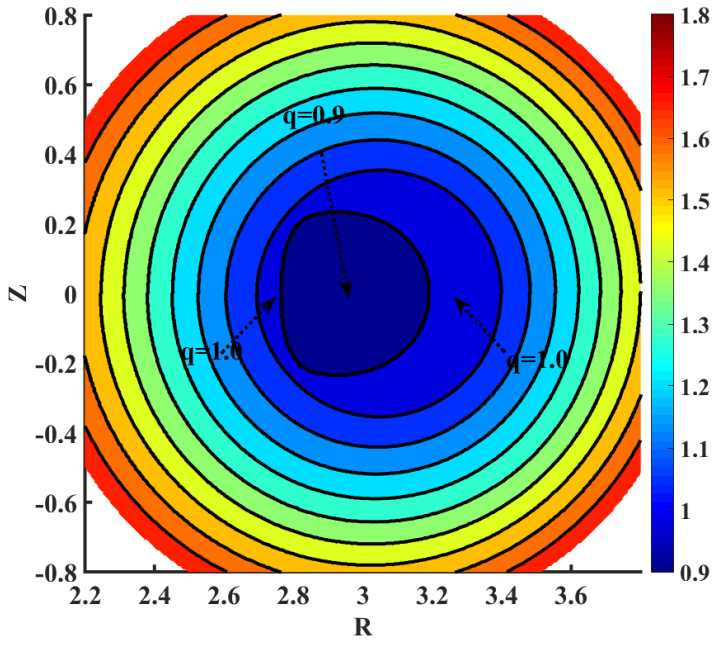

Figure 6 The contour plot of the safety factor at the saturated stage ($t = 4487 t_A$).

B. Influence of the two-fluid effect on the nonlinear behaviors of the resistive-kink mode.

As discussed in Section III.A, the system can evolve into a steady-state with two co-existing 1/1 magnetic islands, and the reconnection is incomplete without the two-fluid effect. However, the steady-state requires the exact symmetry of the secondary magnetic island. When the symmetry is broken, the late nonlinear behaviors of the resistive-kink mode in a low resistivity plasma can be significantly different. In this subsection, we will demonstrate this through the Hall-MHD simulations.

Since the electron diamagnetic frequency $\omega_{*e} = -\frac{d_i m}{\rho r B}\frac{dp_e}{dr}$ and the ion-sound Larmor radius $\rho_s = d_i\sqrt{\mu_0 p / B_0^2}$ are both related to the plasma pressure, the low beta equilibrium is not suitable for investigating the influence of the two-fluid effect. We choose a new equilibrium with the same q profile with Section III. A, but $\beta_0 = 0.011$ (where β_0 is the plasma beta on the magnetic axis). The initial pressure profile is shown in Figure 7. We scan $d_i = 0.001$ to $d_i = 0.03$, and keep other parameters the same as

those in Section III. A. The corresponding electron diamagnetic frequency ω_{*e} changes from 1.7×10^{-5} to 5.1×10^{-4}, which is much smaller than the linear growth rate of the resistive kink mode ($\gamma \sim 2\times10^{-3}$). With those parameters, the two-fluid effect has little influence on the growth rate of resistive-kink mode and only causes the mode structure to slowly rotate in the direction of the electron diamagnetic drift.

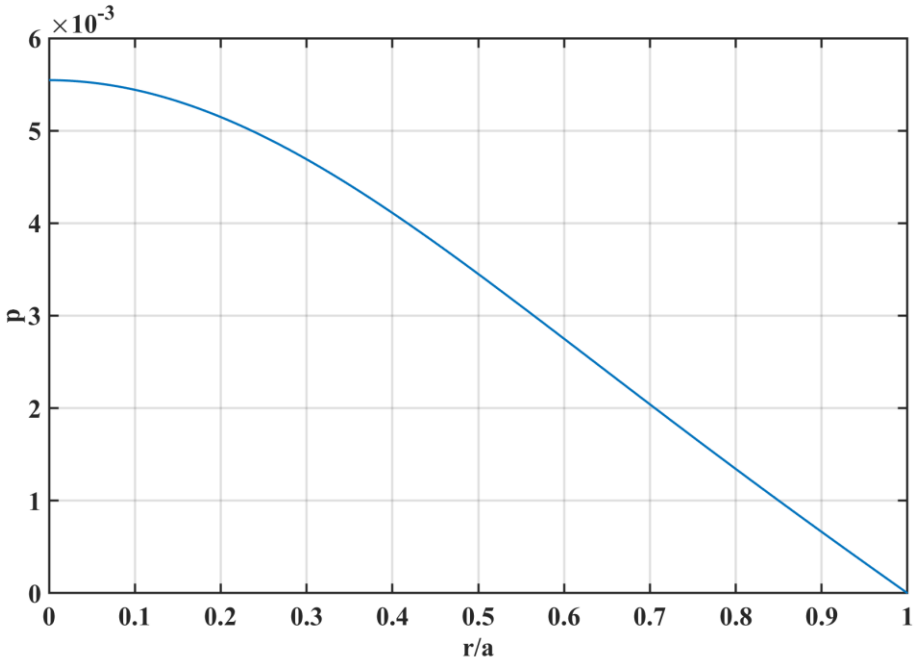

Figure 7 Initial pressure profile used in Section III. B.

Figure 8 shows the four different snapshots of the Poincare plots of the magnetic field for $d_i = 0.001$ ($\omega_{*e} = 1.7\times10^{-5}$): (a) a large secondary island forms, (b) the large secondary island and the main *m*/*n*=1/1 island begin to coalescence, (c) the two magnetic islands almost merges, and (d) the hot core region disappears. Since the two-fluid effect breaks the symmetry, the formation of the large secondary island cannot prevent the further development of the resistive-kink mode as it does in the simulations without the two-fluid effect. With the development of the main *m*/*n*=1/1 magnetic island, the two magnetic islands are finally forced to merge together. After that, the nonlinear behavior of the resistive-kink mode becomes qualitatively the same as that predicted by

Kadomstev's model, and complete reconnection is then observed.

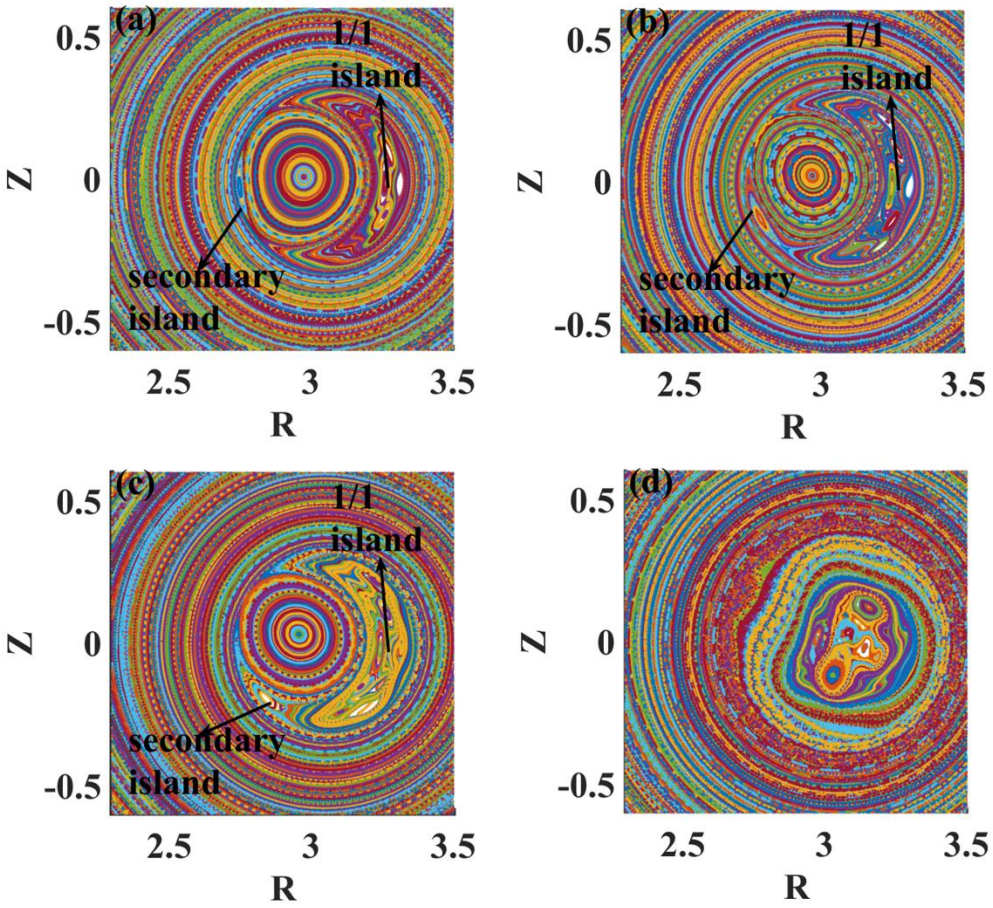

Figure 8 The four different snapshots of the Poincare plots of the magnetic field for $d_i = 0.001$ ($\omega_{*e} = 1.7 \times 10^{-5}$): (a) a large secondary island forms, (b) the large secondary island and the main m/n=1/1 island begin to coalescence, (c) the two magnetic islands almost merges, and (d) the hot core region disappears.

Figures 4 and 8 indicate that the two-fluid effect is important for the reconnection behavior. Without the two-fluid effect, the reconnection will be incomplete if large secondary island forms. However, with the two-fluid effect, the reconnection will always be complete, even if the electron diamagnetic drift frequency is much smaller than the growth rate of the resistive-kink mode. This is because the two-fluid effect breaks the symmetry of the secondary island, and the large secondary island cannot prevent the further development of the resistive-kink mode as it does in the incomplete

reconnection process.

The Poincare plots of the magnetic field at the four typical moments for the simulation with $d_i = 0.03$ ($\omega_{*e} = 5.1\times10^{-4}$) are shown in Figure 9. No large secondary island forms throughout the simulation, and the reconnection process is qualitatively the same as Kadomstev's model. With those parameters, the system enters into the Hall reconnection phase[55], which is similar to that discussed in Ref.[53].

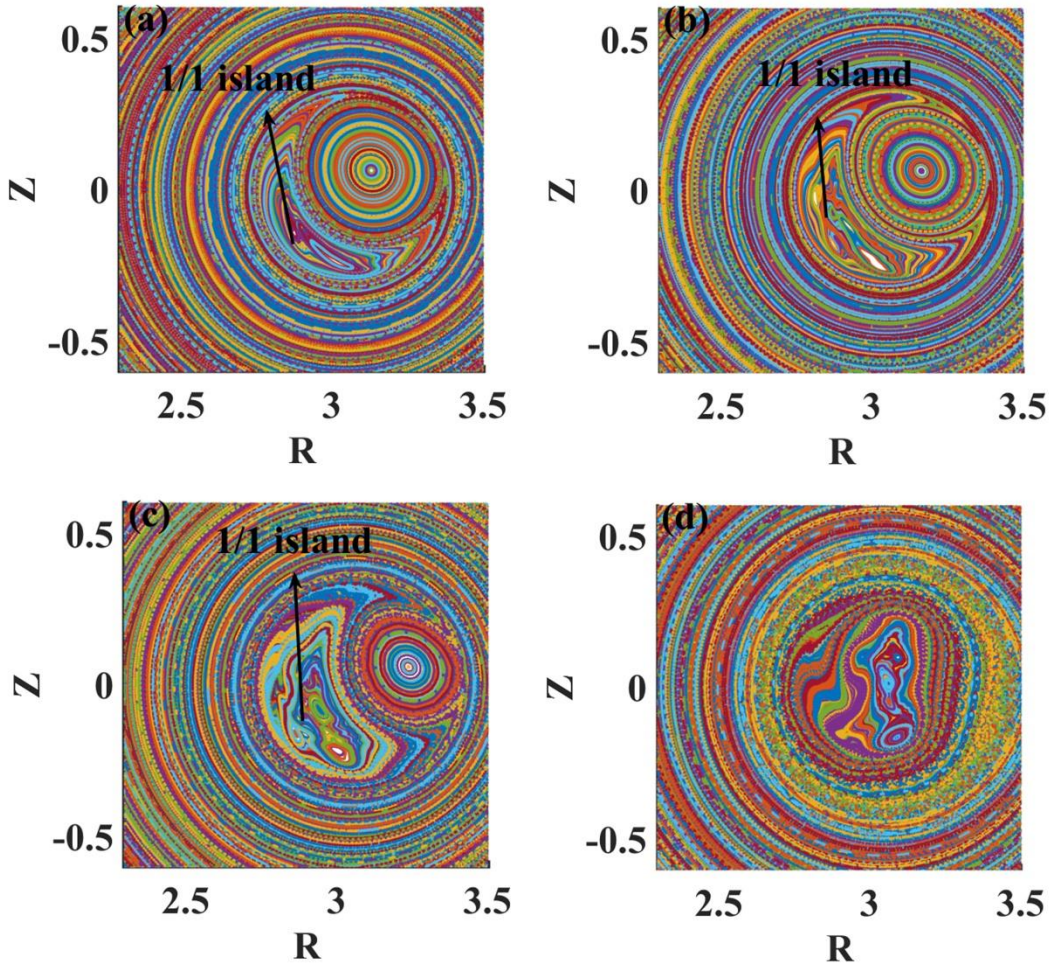

Figure 9 The four typical moments of the Poincare plots of the magnetic field with $d_i = 0.03$ ($\omega_{*e} = 5.1\times10^{-4}$).

C. Influence of the toroidal rotation on the nonlinear behaviors of the resistive-kink mode in the low resistivity plasma

As discussed in Section III.A and B, symmetry is of significant importance for the

nonlinear behaviors of the resistive-kink mode in the low resistivity plasma. In this subsection, we investigate the influence of the toroidal flow on the nonlinear behavior of the resistive-kink mode. We choose an equilibrium with the same q profile as that used in Section III. A, but with the toroidal flow, i.e., $\Omega_0 = 7.5\times10^{-4}$ (where Ω_0 is the toroidal rotation angular velocity on the magnetic axis). The initial Ω profile is shown in Figure 10.

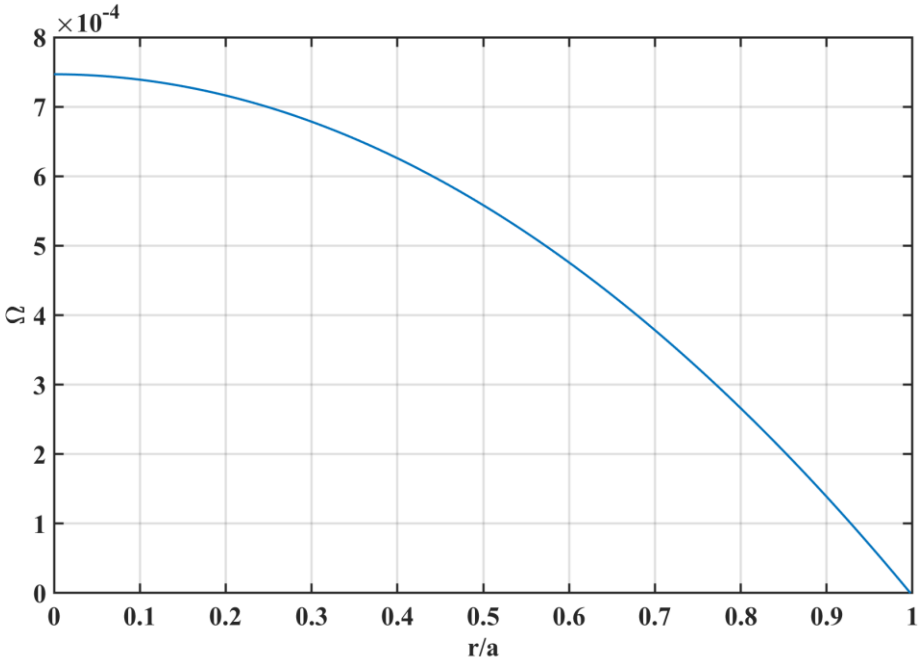

Figure 10 The initial rotation profile used in Section III. C.

Figure 11 shows the four different snapshots of the Poincare plots of the magnetic field for $\Omega_0 = 7.5\times10^{-4}$: (a) a large secondary island forms, (b) the large secondary island and the main m/n=1/1 island begins to coalescence, (c) the two magnetic islands almost merge, and (d)the hot core region disappears completely. Similar to that in Figure 8, the formation of the large secondary island cannot prevent the further development of the resistive-kink mode as it does in the simulations without the toroidal flow and the two-fluid effect. With the development of the main m/n=1/1 magnetic island, the two magnetic islands are finally forced to merge, leading to complete reconnection.

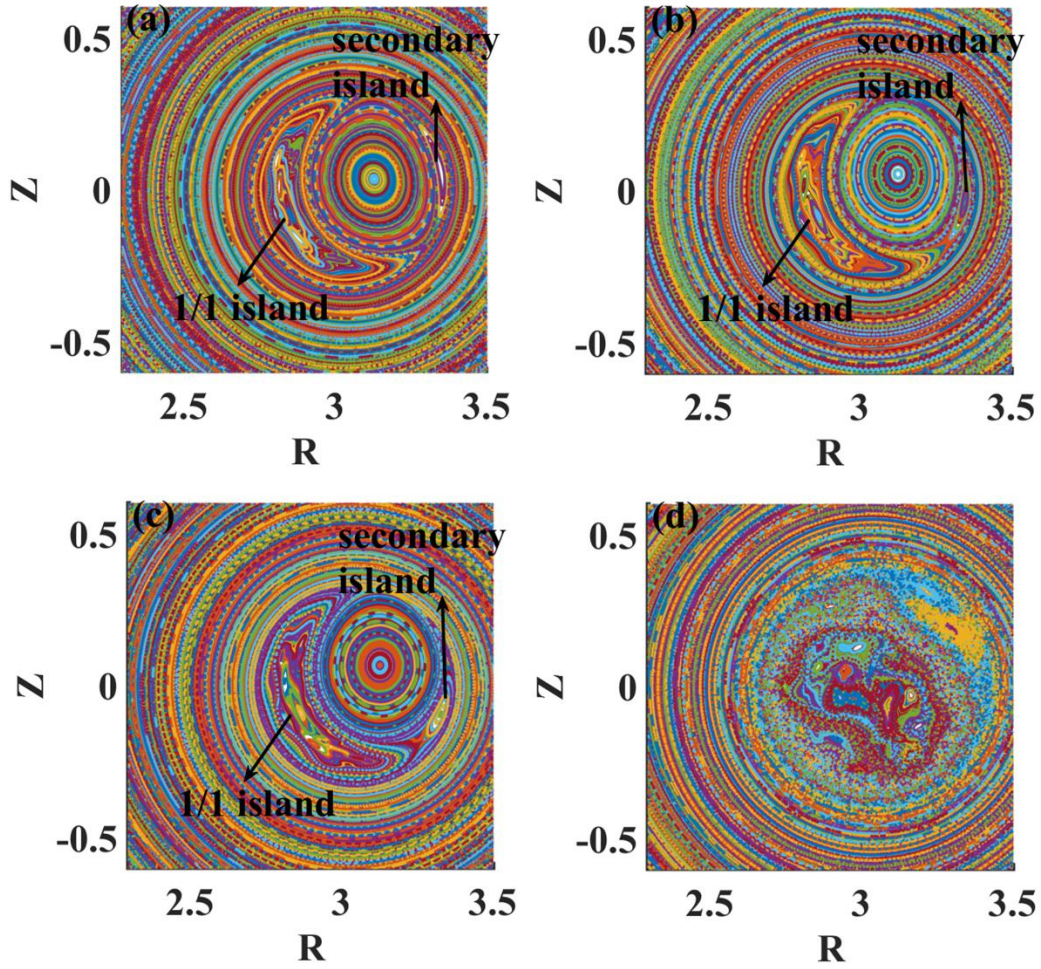

Figure 11 The four different snapshots of the Poincare plots of the magnetic field for $\Omega_0 = 7.5\times10^{-4}$: (a) a large secondary island forms, (b) the large secondary island and the main *m/n*=1/1 island begins to coalescence, (c) the two magnetic islands almost merge, and (d)the hot core region disappears completely.

IV. Discussions and conclusions

Firstly, by following the cylindrical geometry and reduced-MHD simulations by Yu et al. [47], we perform the simulation studies of the incomplete reconnection in the tokamak geometry using the 3D toroidal nonlinear Hall-MHD code CLT. We find that the nonlinear evolution of the resistive-kink mode can be significantly different from Kadomstev's model. With the nonlinear development of the resistive-kink mode, the current sheet becomes thinner and thinner. The secondary tearing instability occurs

when the ratio of the current sheet's length to its thickness reaches a critical value. The current sheet then breaks up, and plasmoids form. The plasmoids eventually merge into a large secondary island, which will finally prevent the further development of the resistive-kink mode. As a result, the system finally evolves into a steady-state with the saturated main *m/n*=1/1 magnetic island and a co-existing large secondary island. The main *m/n*=1/1 magnetic island cannot push the hot core plasma out of the $q<1$ region as it does in Kadomstev's model, which means that the reconnection process is incomplete. Since the hot core remains inside the q=1 surface, the magnetic flux surface around the axis is not destroyed, and the axis's safety factor keeps unchanged throughout the simulation. Our simulation results are well consistent with those from the cylindrical geometry and reduced-MHD simulations.[47]

However, by taking the two-fluid effect and the toroidal flow into account, the nonlinear behaviors of the resistive-kink mode could be largely different. We find that the two-fluid effect and the toroidal flow can break the symmetry of the secondary island. As shown in Section III. B and C, the asymmetry totally destroys the balance between the saturated main *m/n*=1/1 magnetic island and the large secondary island. The further development of the resistive-kink mode forces the large secondary island to be merged into the main *m/n*=1/1 island. After that, the well-developed main *m/n*=1/1 island pushes the hot core plasma out of the $q<1$ region, and all magnetic flux in the central region is reconnected.

Acknowledgment

This work is supported by the National MCF Energy R&D Program No. 2019YFE03090500, the National Natural Science Foundation of China under Grant No. 12005185, 11775188 and 11835010, the Special Project on High-performance Computing under the National Key R&D Program of China No. 2016YFB0200603, Fundamental Research Fund for Chinese Central Universities.

Reference:

[1] S. von Goeler, W. Stodiek, N. Sauthoff, Studies of Internal Disruptions and m=1 Oscillations in Tokamak Discharges with Soft X-Ray Tecniques, Physical Review Letters, 33 (1974) 1201-1203.

[2] K. McGuire, D.C. Robinson, Sawtooth oscillations in a small tokamak, Nuclear Fusion, 19 (1979) 505.

[3] M.A. Dubois, A.L. Pecquet, C. Reverdin, Internal disruptions in the TFR tokamak: A phenomenological analysis, Nuclear Fusion, 23 (1983) 147.

[4] A.W. Edwards, D.J. Campbell, W.W. Engelhardt, H.U. Fahrbach, R.D. Gill, R.S. Granetz, S. Tsuji, B.J.D. Tubbing, A. Weller, J. Wesson, D. Zasche, Rapid Collapse of a Plasma Sawtooth Oscillation in the JET Tokamak, Physical Review Letters, 57 (1986) 210-213.

[5] K. McGuire, V. Arunasalam, C.W. Barnes, M.G. Bell, M. Bitter, R. Boivin, N.L. Bretz, R. Budny, C.E. Bush, A. Cavallo, T.K. Chu, S.A. Cohen, P. Colestock, S.L. Davis, D.L. Dimock, H.F. Dylla, P.C. Efthimion, A.B. Ehrhrardt, R.J. Fonck, E. Fredrickson, H.P. Furth, G. Gammel, R.J. Goldston, G. Greene, B. Grek, L.R. Grisham, G. Hammett, R.J. Hawryluk, H.W. Hendel, K.W. Hill, E. Hinnov, D.J. Hoffman, J. Hosea, R.B. Howell, H. Hsuan, R.A. Hulse, A.C. Janos, D. Jassby, F. Jobes, D.W. Johnson, L.C. Johnson, R. Kaita, C. Kieras-Phillips, S.J. Kilpatrick, P.H. LaMarche, B. LeBlanc, D.M. Manos, D.K. Mansfield, E. Mazzucato, M.P. McCarthy, M.C. McCune, D.H. McNeill, D.M. Meade, S.S. Medley, D.R. Mikkelsen, D. Monticello, R. Motley, D. Mueller, J.A. Murphy, Y. Nagayama, D.R. Nazakian, E.B. Neischmidt, D.K. Owens, H. Park, W. Park, S. Pitcher, A.T. Ramsey, M.H. Redi, A.L. Roquemore, P.H. Rutherford, G. Schilling, J. Schivell, G.L. Schmidt, S.D. Scott, J.C. Sinnis, J. Stevens, B.C. Stratton, W. Stodiek, E.J. Synakowski, W.M. Tang, G. Taylor, J.R. Timberlake, H.H. Towner, M. Ulrickson, S.v. Goeler, R. Wieland, M. Williams, J.R. Wilson, K.L. Wong, M. Yamada, S. Yoshikawa, K.M. Young, M.C. Zarnstorff, S.J. Zweben, High-beta operation and magnetohydrodynamic activity on the TFTR tokamak, Physics of Fluids B: Plasma

Physics, 2 (1990) 1287-1290.

[6] D.J. Campbell, R.D. Gill, C.W. Gowers, J.A. Wesson, D.V. Bartlett, C.H. Best, S. Coda, A.E. Costley, A. Edwards, S.E. Kissel, R.M. Niestadt, H.W. Piekaar, R. Prentice, R.T. Ross, B.J.D. Tubbing, Sawtooth activity in ohmically heated JET plasmas, Nuclear Fusion, 26 (1986) 1085-1092.

[7] O. Sauter, E. Westerhof, M.L. Mayoral, B. Alper, P.A. Belo, R.J. Buttery, A. Gondhalekar, T. Hellsten, T.C. Hender, D.F. Howell, T. Johnson, P. Lamalle, M.J. Mantsinen, F. Milani, M.F.F. Nave, F. Nguyen, A.L. Pecquet, S.D. Pinches, S. Podda, J. Rapp, Control of Neoclassical Tearing Modes by Sawtooth Control, Physical Review Letters, 88 (2002) 105001.

[8] R.J. Buttery, T.C. Hender, D.F. Howell, R.J.L. Haye, O. Sauter, D. Testa, Onset of neoclassical tearing modes on JET, Nuclear Fusion, 43 (2003) 69.

[9] L. Xu, E. Li, T. Zhou, Y. Duan, Y. Huang, H. Lian, S. Wang, J. Liu, Y. Chao, Q. Zang, S. Lin, H. Liu, Z. Luo, H. Wang, L. Zeng, B. Zhang, J. Qian, X. Gong, L. Hu, Observation of helical m/n = 1/1 saturated steady mode in EAST pure electron heating scenario with q0 ≼ 1, Nuclear Fusion, 60 (2020) 106027.

[10] S.C. Jardin, I. Krebs, N. Ferraro, A new explanation of the sawtooth phenomena in tokamaks, Physics of Plasmas, 27 (2020) 032509.

[11] E. Lerche, M. Lennholm, I.S. Carvalho, P. Jacquet, M. Mantsinen, P. Dumortier, D. Van Eester, J.P. Graves, P. Card, C. Noble, Sawtooth control with modulated ICRH in JET-ILW H-mode plasmas, Nuclear Fusion, 60 (2020) 126037.

[12] J. Li, Y. Ding, Q. Yu, N. Wang, D. Li, X. Zhang, D. Han, Z. Chen, Z. Yang, S. Zhou, W. Yan, Y. Liang, X. Zhang, X. Lin, H. Sun, X. Gao, J. Li, Reduction of sawtooth amplitude by resonant magnetic perturbation, Nuclear Fusion, 60 (2020) 126002.

[13] C. Piron, P. Martin, D. Bonfiglio, J. Hanson, N.C. Logan, C. Paz-Soldan, P. Piovesan, F. Turco, J. Bialek, P. Franz, G. Jackson, M.J. Lanctot, G.A. Navratil, M. Okabayashi, E. Strait, D. Terranova, A. Turnbull, Interaction of externaln = 1 magnetic fields with the sawtooth instability in low-qRFX-mod and DIII-D tokamaks, Nuclear Fusion, 56 (2016) 106012.

[14] D. Liu, W.W. Heidbrink, M. Podestà, G.Z. Hao, D.S. Darrow, E.D. Fredrickson, D. Kim, Effect of sawtooth crashes on fast ion distribution in NSTX-U, Nuclear Fusion, 58 (2018) 082028.

[15] B. Somjinda, A. Wisitsorasak, T. Onjun, Impacts of sawtooth crashes on tokamak plasmas in DEMOs, Nuclear Fusion, 60 (2020) 066013.

[16] R. Fischer, A. Bock, A. Burckhart, O.P. Ford, L. Giannone, V. Igochine, M. Weiland, M. Willensdorfer, Sawtooth induced q-profile evolution at ASDEX Upgrade, Nuclear Fusion, 59 (2019) 056010.

[17] Y.-S. Na, Y.H. Lee, C.S. Byun, S.K. Kim, C.Y. Lee, M.S. Park, S.M. Yang, B. Kim, Y.M. Jeon, G.J. Choi, J. Citrin, J.W. Juhn, J.S. Kang, H.S. Kim, J.H. Kim, W.H. Ko, J.M. Kwon, W.C. Lee, M.H. Woo, S. Yi, S.W. Yoon, G.S. Yun, On hybrid scenarios in KSTAR, Nuclear Fusion, 60 (2020) 086006.

[18] C.B. Smiet, G.J. Kramer, S.R. Hudson, Bifurcations of the magnetic axis and the alternating-hyperbolic sawtooth, Nuclear Fusion, 60 (2020) 084005.

[19] W.W. Heidbrink, B.S. Victor, The motional Stark effect diagnostic reliably measures significant deviations in safety factor profile during DIII-D sawteeth, Physics of Plasmas, 27 (2020) 080701.

[20] W. Zhang, Z.W. Ma, F. Porcelli, H.W. Zhang, X. Wang, Sawtooth relaxation oscillations, nonlinear helical flows and steady-state m/n=1 magnetic islands in low-viscosity tokamak plasma simulations, Nuclear Fusion, 60 (2020) 096013.

[21] W. Zhang, Z.W. Ma, H.W. Zhang, J. Zhu, Dynamic evolution of resistive kink mode with electron diamagnetic drift in tokamaks, Physics of Plasmas, 26 (2019) 042514.

[22] G.S. Li, T. Zhang, M.F. Wu, H.M. Xiang, Y.M. Wang, F. Wen, Y. Liu, K.N. Geng, F.B. Zhong, K.X. Ye, Y. Sun, J. Huang, H.Q. Liu, S.B. Zhang, X.D. Lin, X. Gao, Destabilization of field-line localized density fluctuation with a 1/1 internal kink mode in the EAST tokamak, Nuclear Fusion, 59 (2019) 096032.

[23] G.H. Choe, G.S. Yun, H.K. Park, J.H. Jeong, Slow crash in modified sawtooth patterns driven by localized electron cyclotron heating and current drive in KSTAR,

Nuclear Fusion, 58 (2018) 106038.
[24] I. Krebs, S.C. Jardin, S. Günter, K. Lackner, M. Hoelzl, E. Strumberger, N. Ferraro, Magnetic flux pumping in 3D nonlinear magnetohydrodynamic simulations, Physics of Plasmas, 24 (2017) 102511.
[25] Y. Yuan, L. Hu, L. Xu, X. Wang, X. Wang, H. Xu, Z. Luo, K. Chen, S. Lin, Y. Duan, P. Chang, H. Zhao, K. He, Y. Liang, Control of sawtooth via ECRH on EAST tokamak, Physics of Plasmas, 23 (2016) 062503.
[26] A.Y. Aydemir, J.Y. Kim, B.H. Park, J. Seol, On resistive magnetohydrodynamic studies of sawtooth oscillations in tokamaks, Physics of Plasmas, 22 (2015) 032304.
[27] D. Kim, T.P. Goodman, O. Sauter, Real-time sawtooth control and neoclassical tearing mode preemption in ITER, Physics of Plasmas, 21 (2014) 061503.
[28] I.T. Chapman, J.P. Graves, O. Sauter, C. Zucca, O. Asunta, R.J. Buttery, S. Coda, T. Goodman, V. Igochine, T. Johnson, M. Jucker, R.J.L. Haye, M. Lennholm, J.-E. Contributors, Power requirements for electron cyclotron current drive and ion cyclotron resonance heating for sawtooth control in ITER, Nuclear Fusion, 53 (2013) 066001.
[29] I.T. Chapman, R.J. La Haye, R.J. Buttery, W.W. Heidbrink, G.L. Jackson, C.M. Muscatello, C.C. Petty, R.I. Pinsker, B.J. Tobias, F. Turco, Sawtooth control using electron cyclotron current drive in ITER demonstration plasmas in DIII-D, Nuclear Fusion, 52 (2012) 063006.
[30] S.C. Jardin, N. Ferraro, I. Krebs, Self-Organized Stationary States of Tokamaks, Physical Review Letters, 115 (2015) 215001.
[31] C.C. Petty, M.E. Austin, C.T. Holcomb, R.J. Jayakumar, R.J. La Haye, T.C. Luce, M.A. Makowski, P.A. Politzer, M.R. Wade, Magnetic-Flux Pumping in High-Performance, Stationary Plasmas with Tearing Modes, Physical Review Letters, 102 (2009) 045005.
[32] B. Kadomtsev, Disruptive instability in Tokamaks(helical plasma motions), Soviet Journal of Plasma Physics, 1 (1975) 389-391.
[33] A.Y. Aydemir, Nonlinear studies of m=1 modes in high-temperature plasmas, Physics of Fluids B: Plasma Physics, 4 (1992) 3469-3472.

[34] X. Wang, A. Bhattacharjee, Nonlinear dynamics of the m=1 instability and fast sawtooth collapse in high-temperature plasmas, Physical Review Letters, 70 (1993) 1627-1630.

[35] Q. Yu, S. Günter, K. Lackner, Numerical modelling of sawtooth crash using two-fluid equations, Nuclear Fusion, 55 (2015) 113008.

[36] M.T. Beidler, P.A. Cassak, S.C. Jardin, N.M. Ferraro, Local properties of magnetic reconnection in nonlinear resistive- and extended-magnetohydrodynamic toroidal simulations of the sawtooth crash, Plasma Physics and Controlled Fusion, 59 (2017) 025007.

[37] W. Zhang, Z.W. Ma, H.W. Zhang, X. Wang, Role of Hall effect on the resistive kink mode in tokamaks, Plasma Physics and Controlled Fusion, 62 (2020) 025030.

[38] J.A. Wesson, Sawtooth reconnection, Nuclear Fusion, 30 (1990) 2545-2549.

[39] A.J. Lichtenberg, K. Itoh, S.I. Itoh, A. Fukuyama, The role of stochasticity in sawtooth oscillations, Nuclear Fusion, 32 (1992) 495.

[40] J.A. Wesson, Sawtooth oscillations, Plasma Physics and Controlled Fusion, 28 (1986) 243-248.

[41] I.T. Chapman, R. Scannell, W.A. Cooper, J.P. Graves, R.J. Hastie, G. Naylor, A. Zocco, Magnetic Reconnection Triggering Magnetohydrodynamic Instabilities during a Sawtooth Crash in a Tokamak Plasma, Physical Review Letters, 105 (2010) 255002.

[42] A. Kleiner, J.P. Graves, D. Brunetti, W.A. Cooper, F.D. Halpern, J.F. Luciani, H. Lütjens, Neoclassical tearing mode seeding by coupling with infernal modes in low-shear tokamaks, Nuclear Fusion, 56 (2016) 092007.

[43] A. Letsch, H. Zohm, F. Ryter, W. Suttrop, A. Gude, F. Porcelli, C. Angioni, I. Furno, Incomplete reconnection in sawtooth crashes in ASDEX Upgrade, Nuclear Fusion, 42 (2002) 1055.

[44] V. Igochine, J. Boom, I. Classen, O. Dumbrajs, S. Günter, K. Lackner, G. Pereverzev, H. Zohm, A.U. Team, Structure and dynamics of sawteeth crashes in ASDEX Upgrade, Physics of Plasmas, 17 (2010) 122506.

[45] F. Porcelli, D. Boucher, M.N. Rosenbluth, Model for the sawtooth period and

amplitude, Plasma Physics and Controlled Fusion, 38 (1996) 2163.

[46] M.T. Beidler, P.A. Cassak, Model for Incomplete Reconnection in Sawtooth Crashes, Physical Review Letters, 107 (2011) 255002.

[47] Q. Yu, S. Günter, K. Lackner, Formation of plasmoids during sawtooth crashes, Nuclear Fusion, 54 (2014) 072005.

[48] H.W. Zhang, J. Zhu, Z.W. Ma, G.Y. Kan, X. Wang, W. Zhang, Acceleration of three-dimensional Tokamak magnetohydrodynamical code with graphics processing unit and OpenACC heterogeneous parallel programming, International Journal of Computational Fluid Dynamics, 33 (2019) 393-406.

[49] W. Zhang, Z.W. Ma, S. Wang, Hall effect on tearing mode instabilities in tokamak, Physics of Plasmas, 24 (2017) 102510.

[50] L. Duan, X. Wang, X. Zhong, A high-order cut-cell method for numerical simulation of hypersonic boundary-layer instability with surface roughness, Journal of Computational Physics, 229 (2010) 7207-7237.

[51] C. Cheng, M. Chance, NOVA: A nonvariational code for solving the MHD stability of axisymmetric toroidal plasmas, Journal of Computational Physics, 71 (1987) 124-146.

[52] A.Y. Aydemir, J.C. Wiley, D.W. Ross, Toroidal studies of sawtooth oscillations in tokamaks, Physics of Fluids B: Plasma Physics, 1 (1989) 774-787.

[53] S. Günter, Q. Yu, K. Lackner, A. Bhattacharjee, Y.M. Huang, Fast sawtooth reconnection at realistic Lundquist numbers, Plasma Physics and Controlled Fusion, 57 (2015) 014017.

[54] A. Bhattacharjee, Y.-M. Huang, H. Yang, B. Rogers, Fast reconnection in high-Lundquist-number plasmas due to the plasmoid Instability, Physics of Plasmas, 16 (2009) 112102.

[55] Y.-M. Huang, A. Bhattacharjee, B.P. Sullivan, Onset of fast reconnection in Hall magnetohydrodynamics mediated by the plasmoid instability, 18 (2011) 072109.